

Three-Stage Predictive Warning System for Human Takeover in Automated Inland Vessels

1st Thomas Jan Hornig
Institute of Automatic Control
RWTH Aachen University
Aachen, Germany
t.hornig@irt.rwth-aachen.de

2nd Markus Mizael Moser
Institute of Automatic Control
RWTH Aachen University
Aachen, Germany
m.moser@irt.rwth-aachen.de

3rd Ros Lisha Fernandez
Institute of Automatic Control
RWTH Aachen University
Aachen, Germany
lisha.fernandez@rwth-aachen.de

4th Heike Vallery
Institute of Automatic Control
RWTH Aachen University
Aachen, Germany
h.vallery@irt.rwth-aachen.de

5th David Stenger
Institute for Data Science
in Mechanical Engineering
RWTH Aachen University
Aachen, Germany
david.stenger@dsme.rwth-aachen.de

Abstract—Current track-keeping systems used on real-world inland vessels do not consider obstacles and the fairway boundary and, therefore, cannot perform evasive maneuvers to avoid obstacles. Because of that, human operators must keep paying attention to anticipate critical situations to take over manual control. However, due to the high inertia of the underactuated inland vessels, it is difficult to estimate when it is too late to intervene. For this purpose, we propose a warning system that continuously estimates the risk of an inland vessel with a track-keeping system regarding possible collisions with obstacles and fairway violations. Depending on the assessed risk, a warning is given early enough to the shipmaster so that there is enough time to take back steering safely. The Warning System has a three-stage sequential structure. First, the vessel’s position is predicted at a future time step to consider the time delay a human introduces by assessing the situation and planning the next action. Secondly, an Optimal Control Problem is solved with implemented collision avoidance and fairway compliance constraints to determine an optimal trajectory for the vessel. Afterward, the calculated trajectory is post-processed by assessing the safety to give out an estimation of the current warning level. The proposed warning system is tested using a Matlab/Simulink simulation on three safety-critical scenarios.

Index Terms—Marine safety, Risk assessment, Prediction methods, Warning systems, Trajectory planning

I. INTRODUCTION

Research on (semi)-automated ships and the development of assistance systems for inland vessels is driven by potential improvements regarding fuel efficiency and safety, as well as alleviating the burden on shipmasters. In the inland waterway transportation sector, track-keeping systems for inland vessels that can support human operators and guide the vessel along a predetermined path are already used on some ships. However, these systems often do not adapt the path when traveling and do not consider obstacles.

*This work was supported by the Federal Ministry for Digital and Transport, Germany, as part of the research project "SAFEBin" (FKZ-45DTW2V05C). Responsibility for the content of this publication lies with the author.

One solution to simultaneously reduce the burden on shipmasters and increase overall safety is to continuously supervise the ship’s current situation and surroundings with a warning system that can predict upcoming dangerous scenarios. If the estimated risk becomes too large, a warning is given early enough so that a shipmaster has enough time to react to the dangerous situation.

Risk assessment for maritime vessels has a long history of research, with many different methods for overseeing a ship and evaluating the current risk of a collision.

A popular approach for traffic situations with multiple ships is to use the Distance to Closest Point of Approach (DCPA) and Time to Closest Point of Approach (TCPA). In [1], a linear combination, and in [2], the Euclidean distance of the DCPA and TCPA is used to calculate the current collision risk.

The use of fuzzy logic is another widespread proposal. These are built on experts’ knowledge, such that the risk assessment can implement the experience of human operators. Different factors like DCPA, TCPA, environmental conditions, the ship’s current speed, and more are taken as inputs to this logic to generate an estimate of the current risk [3] [4]. To further consider human factors, models like Bayesian belief networks are used for the risk assessment [5].

In addition, model predictive trajectory planners and controllers have been proposed for autonomous vessels to find safe trajectories that avoid paths that lead to collisions [6] [7]. Different methods exist to determine the safety of the calculated trajectories. This is often done in a post-processing step where the trajectories of all moving entities are evaluated with respect to whether and how likely a collision is about to happen [8].

However, these aforementioned methods are not primarily designed for a warning system (WS) for inland vessels with a simple track-keeping system used in industry.

Therefore, we propose a dedicated warning system based on a model predictive trajectory planner that considers this

use case's critical factors. As a primary addition to previous work, the proposed system considers the preparation time a human needs to take over control, perceive the risky situation, and decide the next action after a warning. In addition, the system distinguishes three different warning levels, which are tailored to the use case of an automated inland vessel.

For the risk assessment, the WS is using a sequential three-stage structure. Firstly, the ship's position where a human can act after a takeover is approximated. Subsequently, a nonlinear program (NLP) is solved to find a feasible trajectory, with the estimated position as the initial state. The ship's dynamic, obstacle, and boundary constraints are implemented in the NLP to consider those factors. Lastly, the calculated trajectory is examined by checking which conditions are fulfilled for one of the warning levels.

This paper is structured as follows. Section II describes the used ship model. Section III presents the inner mathematical structure of the WS and the condition for the different warning levels. The approach is tested using simulations in Section IV. The paper closes with an evaluation of the simulation results and an outlook in Section V.

II. SHIP MODEL

The optimal trajectory, calculated by the WS, has to consider the real vessel's dynamics and limitations. For that reason, a ship model is used, which is later implemented in the Optimal Control Problem of the WS. The dynamics of an inland surface vessel in calm water conditions can be described using the following 3-degrees of freedom model:

$$\begin{aligned} \dot{\eta} &= \mathbf{R}(\psi)\boldsymbol{\nu} \\ \mathbf{M}\dot{\boldsymbol{\nu}} + \mathbf{C}(\boldsymbol{\nu})\boldsymbol{\nu} &= \boldsymbol{\tau} \end{aligned} \quad (1)$$

The generalized position vector $\boldsymbol{\eta} = [x, y, \psi]^T$ contains the center position x and y and the heading angle ψ of the ship. The generalized velocity vector in a body-fixed frame is $\boldsymbol{\nu} = [u, v, r]^T$ with surge and sway velocity u and v as well as the yaw rate r . The matrices \mathbf{M} and \mathbf{C} are the Inertia- and Coriolis matrices, respectively, as per [9]. The vector $\boldsymbol{\tau} = [X, Y, N]^T$ describes the forces acting on the vessel, which strongly depend on the current rudder deflection angle δ . These forces are approximated by using the Abkowitz approach with Taylor series up to the third order. The non-dimensional formulation of the external forces and the values for the used hydrodynamic coefficients are recited in [10].

The model assumes a constant shaft power, reflected via a nominal surge velocity U_0 , which is a common steering behavior of inland vessels as power changes while traveling through the waterways are rare. Therefore, the only way to influence the vessel in the model is by changing the setpoint of the rudder deflection angle δ_{sp} . As a result, no changes in velocity are possible for the planned trajectory. This increases the safety margin of the WS because a shipmaster who takes over has the additional freedom to engage a breaking maneuver. The rudder dynamics are approximated as:

$$\dot{\delta} = \frac{1}{T_\delta} \cdot (\delta_{sp} - \delta) \quad (2)$$

The time constant T_δ specifies the rate of the dynamic. With that, the state vector of the vessel \boldsymbol{x} is composed of the generalized position $\boldsymbol{\eta}$, the velocity vector $\boldsymbol{\nu}$ and the rudder deflection angle δ . Lastly, the maximum angle of the rudder δ_{\max} and the maximum rate of change of the rudder angle Δ_{\max} are subject to constraints.

III. WARNING SYSTEM

A. Structure of Warning System

The purpose of the warning system is to give a continuous risk assessment for an inland vessel with a track-keeping system used in industry. The ship, which will be supervised by the warning system, is assumed to be controlled by a simple path-following controller, which does not consider obstacles or the fairway. Fig. 1 shows the structure of an automated ship with a controller and the added warning system. The WS requires no information from the controller except the reference path. This makes the WS more compatible with different controllers. Additionally, the WS receives the measurement of the current vessel state \boldsymbol{x} and the perception data of the surroundings. To detect obstacles and the fairway, the vessel needs added sensors to enable the consideration of these boundaries.

The sequential structure of the WS is as follows: First, the WS predicts the ship's position after the preparation time to account for where the vessel will be when a shipmaster is ready to control it. After this, the WS solves an Optimal Control Problem to calculate a feasible trajectory for a fixed number of future time steps defined by the prediction horizon. The predicted position is the starting point, and constraints are implemented to comply with the obstacle avoidance and the fairway boundaries. For this optimization problem, the vessel geometry in the constraints is enlarged to account for uncertainties like a model plant mismatch or disturbances. After the NLP is solved for the current time step, the calculated trajectory from the Optimal Control Problem (OCP) is post-processed. It is checked whether the vessel needs to perform an evasive maneuver and if the safety buffer defined by a ship domain is large enough. Depending on this, different warning levels will be given. In the following, the consideration of the preparation time is first described. Next, the different enlarged vessel geometries are introduced. Subsequently, the fairway compliance and obstacle constraints, as well as the cost function of the NLP, are presented. At the end, the post-processing step and the warning levels are described.

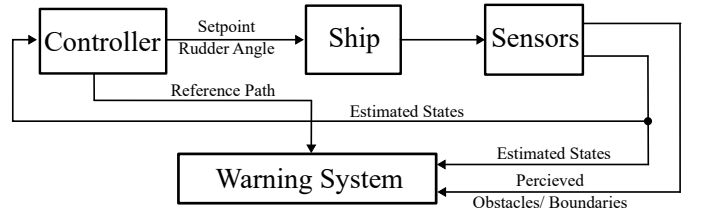


Fig. 1. Implementation of the warning system into the control structure of an automated ship

B. Consideration of Preparation Time for Take Over

When the warning system issues an alarm, it takes a shipmaster some time to get to the control station, assess the critical situation, and plan the next action. This time delay is combined to the needed preparation time T_{prep} that has to be accounted for in the WS so that a person has enough time to react to a warning before the critical scenarios become unsolvable. The preparation time strongly depends on the complexity of the current scenario as described in [11]. Because the WS is working in discrete time, the possibility exists that a critical scenario happens just after a time step and is first noticed at the next time step. Additionally, a warning for a critical situation can first be given when the calculations to solve the NLP are finished. To compensate for these effects, one time step of the WS T_s and a buffer for the maximum expected calculation duration T_{buffer} are added to the preparation time T_{prep} to determine the needed safety time T_{safety} the WS has to consider:

$$T_{\text{safety}} = T_{\text{prep}} + T_s + T_{\text{buffer}} \quad (3)$$

To incorporate T_{safety} in the WS, it is assumed that the ship's path tracking controller keeps the vessel on the reference path with the nominal surge velocity U_0 for the duration of T_{safety} . With that assumption, the ship's position on the reference path after this time is calculated. This predicted future state $\bar{\mathbf{x}}_k$ is then used as the initial point for the OCP. Thus, when the OCP detects a critical situation in the future and a warning is issued, the shipmaster still has the time T_{safety} to react to the situation accordingly.

C. Safety Area and Ship Domain

To increase the safety margin of the WS, a safety area and a ship domain are defined around the vessel. These safety buffers are crucial because errors in state estimation and perception, as well as a model plant mismatch and disturbances, will lead to a difference between the eventual real-world positions of the ego vessel and obstacle vessel compared to their predicted positions.

The different areas and their corresponding dimensions are shown in Fig. 2. The gray rectangle represents the real geometry of the ship with defined length l and width w . The blue

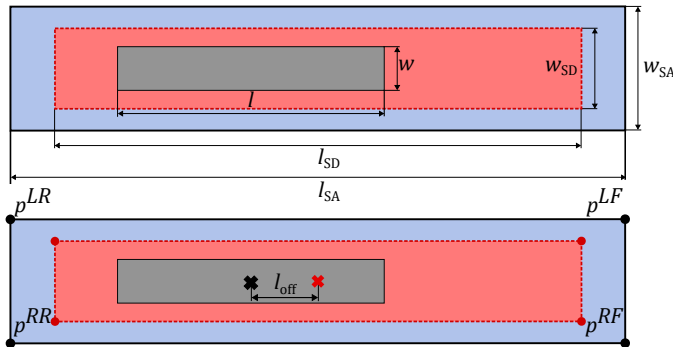


Fig. 2. Illustration of the safety area and the ship domain around the real geometry of the ship

area describes the safety area of the with the enlarged length l_{SA} and width w_{SA} . This area and the corresponding labeled corner points are used in the formulation of the constraints for the NLP where slight violations are allowed. The red area represents the ship domain, which describes the area around the ship, defined by the length l_{SD} and the width w_{SD} , which should stay completely free of any obstacles or boundaries during the whole operation of the vessel. The ship domain is not considered inside the NLP formulation to reduce the complexity of the NLP. After solving for an optimal solution using NLP, the ship domain is tested for violation of the constraints. The center of the safety area and ship domain is shifted towards the front of the ship by the length l_{off} because the possible uncertainties for the position are largest in the direction of the ship's velocity.

The area of the vessel's geometry, ship domain, safety area, and obstacles are modeled individually as rectangles. An area occupied by a rectangle can be described by all \mathbf{x} that satisfy:

$$\mathbf{A}\mathbf{x} \leq \mathbf{b} \quad (4)$$

Where the matrix $\mathbf{A} \in \mathbb{R}^{4 \times 2}$ contains the normal vectors of the sides and the entries in the vector $\mathbf{b} \in \mathbb{R}^4$ specify the boundary of the respective half space. \mathbf{A} and \mathbf{b} can be calculated from a base geometry, which is chosen to be the area of the unrotated shape with its center at the origin and which is defined by $\tilde{\mathbf{A}}\mathbf{x} \leq \tilde{\mathbf{b}}$ as in [12]. For an arbitrary center position \mathbf{p} and heading angle ψ , \mathbf{A} and \mathbf{b} can then be calculated using

$$\mathbf{A} = \tilde{\mathbf{A}}\mathbf{R}^T(\psi), \quad \mathbf{b} = \tilde{\mathbf{b}} + \mathbf{A}\mathbf{p}. \quad (5)$$

Lastly, the position of a point \mathbf{p}^i on the ship or the enlarged domain, e.g. a corner point, can be calculated using the ship's center position \mathbf{p} and heading angle ψ as:

$$\mathbf{p}^i = \mathbf{p} + \mathbf{R}(\psi)\mathbf{d} \quad (6)$$

where $\mathbf{d} = [d_x, d_y]^T$ contains the offset in x and y direction from \mathbf{p} to \mathbf{p}^i in the local coordinate system of the vessel.

D. Boundary and Obstacle Constraints

Different formulations for the constraints of the fairway and the obstacle constraints are chosen. To enforce fairway compliance, the vertices of the ship's safety area are checked against the connected areas of super ellipses, which model the area outside the fairway boundaries. For obstacle avoidance, a differentiable reformulation of the signed distance between the ego ship (ES) and an obstacle is used [12].

The formulation for the boundary constraints is similar to [13] and will be presented in the following. In general, the area covered by a super ellipse A_{SE} can be formulated as

$$A_{\text{SE}} = \{ \mathbf{x} \in \mathbb{R}^2 \mid f_{\text{SE}}(\mathbf{x}) \leq 1 \} \quad (7)$$

with

$$f_{\text{SE}}(\mathbf{x}) = \left(\frac{\cos(\alpha) \cdot (x - x_m) + \sin(\alpha) \cdot (y - y_m)}{a} \right)^{2n} + \left(\frac{-\sin(\alpha) \cdot (x - x_m) + \cos(\alpha) \cdot (y - y_m)}{b} \right)^{2n} \quad (8)$$

where x_m, y_m, a, b, α describe the midpoint, length of semi-axes and orientation of the superellipse. With the parameter n , the shape of the superellipse can be influenced. For $n = 1$, the super ellipse equals a normal ellipse, and the shape becomes more rectangular for larger values.

Using smooth Constructive Solid Geometry (CSG), the smoothly approximated area A_U of the union of m individual superellipses, defined by $f_{SE,i}, i = 1, \dots, m$, can be formulated as [14].

$$A_U = \left\{ \mathbf{x} \in \mathbb{R}^2 \mid U(\mathbf{x}) = \left(\sum_{i=1}^m (f_{SE,i}(\mathbf{x})^{-p}) \right)^{-\frac{1}{p}} \leq 1 \right\} \quad (9)$$

For larger values of the parameter p , the smooth approximation of the combined area becomes more accurate. Two functions, U_L and U_R , defining a continuous and smooth area outside the left and right fairway boundary, respectively, can be constructed using (9). These functions correspond to the approximated union of the area of the individual super ellipses applied to the respective fairway polygon chain line. To decrease the complexity of the boundary constraints, a filter is implemented to consider only the union of relevant super ellipses for the current prediction horizon during the optimization. The four vertices of the outer safety area of the ship are checked in the NLP to see if they are within the modeled area and, therefore, within the fairway. Furthermore, the constraints are scaled logarithmically to improve the scaling and numeric stability of the optimization problem.

To have a reliable WS, the NLP should never become infeasible, even during critical situations. To ensure that a feasible solution always exists, the boundary and obstacle constraints are relaxed using the slack variables ϵ .

$$\begin{aligned} \log(U_L(\mathbf{p}^{LF})) &> -\epsilon_{LF}, & \log(U_R(\mathbf{p}^{RF})) &> -\epsilon_{RF}, \\ \log(U_L(\mathbf{p}^{LR})) &> -\epsilon_{LR}, & \log(U_R(\mathbf{p}^{RR})) &> -\epsilon_{RR} \end{aligned} \quad (10)$$

The positions of the vertices are calculated using (6). For more information about the NLP constraint formulation for the fairway compliance, see [13].

For obstacle avoidance, the geometries of the ES and the obstacles are assumed to be rectangular, and their covered areas can be described via the inequality (4). In the following, \mathbf{A}, \mathbf{b} are used for the obstacle geometry and \mathbf{C}, \mathbf{d} for the geometry of the ES. The collision avoidance constraint formulated as a dual reformulation of the signed distance is then:

$$\begin{aligned} \frac{\boldsymbol{\lambda}^T \mathbf{d} + \boldsymbol{\mu}^T \mathbf{b}}{\|\mathbf{A}^T \boldsymbol{\mu}\|} &\leq \epsilon_{\text{Obst}} \\ \mathbf{C}^T \boldsymbol{\lambda} + \mathbf{A}^T \boldsymbol{\mu} &= \mathbf{0} \\ \boldsymbol{\lambda}, \boldsymbol{\mu} &\geq \mathbf{0} \end{aligned} \quad (11)$$

Where $\boldsymbol{\lambda}$ and $\boldsymbol{\mu}$ are additional optimization variables introduced to the nonlinear program. Analogous to the boundary constraints, slack variables ϵ_{Obst} are introduced for each obstacle to ensure the feasibility of the NLP. If a $\boldsymbol{\lambda}$ and $\boldsymbol{\mu}$ are found that satisfy (11), the two objects do not overlap and therefore do not collide. For more information on the dual formulation of the signed distance function, see [12].

E. Cost Function

The cost function J of the NLP consists of three terms:

$$J = J_{\text{ct}} \cdot q + \sum_{k=0}^{N-1} (u_k - u_{k-1})^2 \cdot r + \|\boldsymbol{\epsilon}_k\|_1 \cdot m \quad (12)$$

The second part of the cost function is a regularization term for the change of the input. The third term is used to penalize the slack variables ϵ with respect to the 1-norm, such that the collision avoidance and fairway compliance constraints are only relaxed when no other feasible trajectory can be found for the respective domain. The weighting factors q, r , and m are added to influence the impact of each term.

The first term J_{ct} is implemented to penalize a deviation from the preplanned path that will eventually be tracked by the vessel's path following controller. This is necessary so that the WS assesses the risk around the upcoming reference path segments before the ship actually reaches these segments. For this, the relevant waypoints for the prediction horizon are determined each time the WS is called. Path following for the upcoming path segment after $\bar{\mathbf{x}}_k$ is achieved by the following term:

$$J_{\text{ct}} = \sum_{k=1}^N \det([\mathbf{s}_k, \mathbf{r}_k]^2) \quad (13)$$

To enhance readability, the index k is omitted in the following. The reference vector \mathbf{r} starts at \mathbf{w}_a , has the direction towards \mathbf{w}_b , and is normalized. The waypoints \mathbf{w}_a and \mathbf{w}_b describe a corresponding path segment, e.g. the line from \mathbf{w}_a to \mathbf{w}_b . The vector \mathbf{s} also starts at \mathbf{w}_a and points to the bow of the ship \mathbf{p}^b . Since both \mathbf{r} and \mathbf{s} share the same starting point and the reference vector is normalized, this formulation corresponds to the cross-track error from the bow \mathbf{p}^b to the respective reference path segment. During steering, the ship's center experiences a nonminimal phase behavior, which can be reduced by tracking the bow instead of the ship's center. Further information about the formulation of the cross-track error is given in [13].

F. Alarm Condition of the Warning System

After the OCP is solved, the resulting trajectory from the NLP solution is post-processed to assess the current risk. For this purpose, the calculated trajectory, slack variables, position, and dimension for the obstacles and fairway are considered.

When the slack variables are zero, and the resulting trajectory follows the reference path closely, the warning level is set to green. As in this case, the OCP did not need to perform an evasive maneuver, and there was enough distance to the obstacles and the fairway boundary. When the slack variables are zero, but the resulting trajectory has a high cross-track error J_{ct} , the vessel must perform an evasive maneuver. In this case, the risk level is set to yellow. The shipmaster should be ready to intervene soon, as the vessel's track-keeping system may face a situation it cannot handle.

If the slack variables exceed zero, the resulting OCP trajectory for the safety area could not satisfy the NLP's fairway or collision avoidance constraints. To distinguish the risk in

this case, it is checked whether the ship domain is also violated. To check this, the corner points of the ship domain for the resulting trajectory from the NLP are again checked for condition (10). As this is done after the NLP, the condition (10) is now checked for strict > 0 because no slack variables are used now. Additionally, the corner points of the vessel and the individual obstacles are tested for lying inside the obstacles or the vessel respectively with equation (4). If, after these checks, the fairway boundary and obstacle are only inside the safety area but not inside the ship domain, the risk level is set to yellow, and the shipmaster should be ready to take over. If the ship domain violates any constraints, the warning level is set to red, and the shipmaster should immediately take over control from the track-keeping system as a safety critical situation is ahead. This line of action is shown for one prediction step in Fig. 3. In the depicted example, the safety area's black border crosses the waterway's boundary, which is modeled with the union of the shown superellipses in red. This scenario is possible as an optimal solution for the NLP because of the slack variables. The risk level is set to the yellow warning level for the example shown because the internal ship domain does not violate the boundary constraint.

IV. SIMULATION

This section tests the warning system for different scenarios in a Matlab/Simulink simulation. First, the parameters used for the simulations are given. Then, this section presents the different simulation test cases and results.

A. Simulation Structure

The used vessel model has a length of $l = 105$ m and a width of $w = 9.5$ m. The length l_{SD} and width w_{SD} of the ship domain are twice the length and width of the real ship geometry. For the safety area, a factor of 2.5 is chosen for the length l_{SA} and the width w_{SA} . The offset length l_{off} is set to one-quarter of the ship's length l . For the rudder constraints, the values $\delta_{max} = (\pm)30$ deg and $\Delta_{max} = (\pm)10$ deg s $^{-1}$ are used and the time constant of the rudder dynamic is $T_\delta = 2$ s. The constant surge speed of the ship is $U_0 = 2.5$ ms $^{-1}$. Following the results of [11], the preparation time is set to $T_{prep} = 40$ s. An update time step of $T_s = 5$ s and a buffer of $T_{buffer} = 5$ s is chosen. Consequently, with (3) T_{safety} is set to

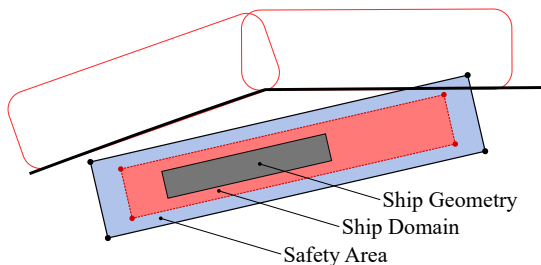


Fig. 3. Representation of the warning condition regarding the safety area and the ship domain in combination with the super ellipses used for the formulation of the boundary constraints. Here, two individual super ellipses are shown and not the resulting unified area after the smooth CSG approximation

50 s. The prediction horizon N is 40. With the nominal surge velocity U_0 and the update time T_s , the length overseen by the WS is therefore equal to 500 m. The weighting matrices q and r are equal to the identity matrix, and the weighting factor for the slack variables m is set to 10^5 . For the fairway modeling, the shape parameter of the superellipses n in (8) and the smooth constructive solid geometry parameter p in (9) are set to 2.

The NLP is formulated using the multiple shooting method and implemented using CasADi [15] with the RK4 integration method. The Interior Point Optimizer IPOPT [16] is utilized to solve the NLP at every update step of the WS, with the initial guess of the shifted previous iteration.

B. Simulation Test Cases

In the upcoming simulations, an automated vessel steered by a path-following controller that does not react to upcoming obstacles and boundaries of the fairway is simulated. The WS does not directly interfere with the controller but assesses the current risk level. Three test cases are used to test the proposed warning systems for different scenarios where human intervention is needed. The used fairway boundary is based upon real-world data from the Rhine River in Germany. In the first test case, a head-on situation is tested. In this scenario, the ego ship is driving along the middle of the waterway, and a moving obstacle ship (OS) is approaching the ES. The OS has the same dimensions and surge velocity as the ES. For obstacle constraints of the OS, the dimensions for the ship domain are used such that the domains of both ships are never allowed to intersect. The controller of the ES follows the preplanned path and does not react to the approaching obstacle. In Fig. 4, the time step, where the warning level is set to red, is shown. The ship's current position with the ship domain and safety area is shown. Furthermore, the current position of the OS is given in dark gray. The red line indicates the reference path the controller of the ego ship follows. The blue line is the trajectory that the WS calculates. This trajectory tries to avoid the upcoming OS and returns to the reference path after the critical situation. The markers on the blue line denote the ship's center for every prediction step of the NLP solution. There is a distance between the ship's center and the blue markers because the formulation compensates for the preparation time. Additionally, Fig. 4 displays the violation of the predicted ship domains of the ego in light red and obstacle ship light gray. For the presented situation, the WS can no longer find a feasible trajectory that does not violate the ship domains. Consequently, the WS gives out a red warning level. A yellow warning level is given far beforehand because the WS has already calculated an evasive trajectory that deviates from the preplanned path in previous time steps.

The second scenario tests an overtaking scenario with a slower obstacles ship driving in the same direction. Simultaneously, a second OS approaches the ego ship at the same surge speed as the ES. In Fig. 5, the time step where the WS sends out an alarm and the prediction step where the ship domains are violated are shown. The computed trajectory of the WS

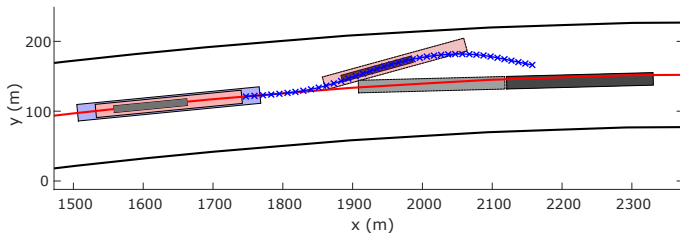


Fig. 4. First test case: head-on scenario between ego ship and obstacle ship

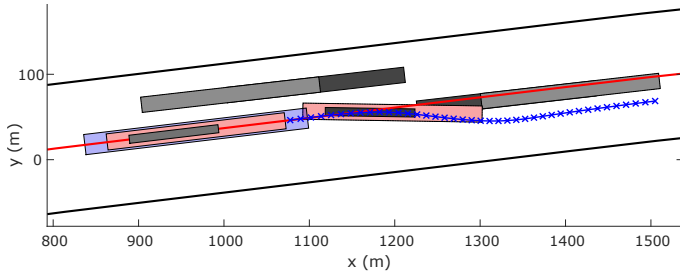


Fig. 5. Second test case: simultaneous overtaking and head-on scenario, with a potential rear-end collision

tries to overtake the first OS on the starboard side because the port side will be occupied by the upcoming OS. However, the controller is just tracking the path and is, therefore, getting closer to the first slower OS. The ES is too close to the first OS for the shown time step, so no safe trajectory can be found. This is also displayed in Fig. 5, where the predicted ship domain of the OS in light red overlaps the predicted ship domain of the ES in light gray. With that, the warning level is set to red, and an alarm is given.

The third test case describes a scenario where a static obstacle blocks the complete fairway. Because of the constant speed of the ES, the WS takes no braking action into account. In Fig. 6, the time step where an alarm is issued is illustrated. At the time steps shown, the vessel gets so close to the obstacle that a violation of the obstacle or boundary constraints is unavoidable. The violation of the ship domain with the fairway boundary is shown in Fig. 6.

V. EVALUATION AND OUTLOOK

The simulations for the three different test cases show that the proposed warning system can detect different risky situations before they actually occur and in time for a human to intervene. The system's large foresight allows an alarm to be given early in advance. Especially in the scenario where an obstacle is blocking the whole fairway, this foresight is crucial because it allows a shipmaster to take over control of the ship in time to initiate a braking maneuver. Future work will address the implementation of uncertainties in the state estimation and the perception of obstacles and boundaries. Furthermore, implementing a COLREGS-compliant planned trajectory could improve the warning system's applicability.

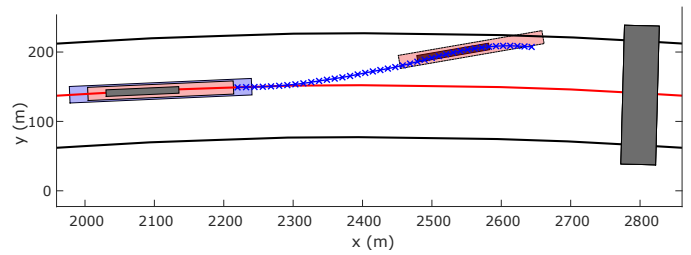


Fig. 6. Third test case: ego ship approaches an obstacle blocking the fairway

REFERENCES

- [1] Won-Sik Kang, Young-Soo Park, and Jeong-Bin Yim, "Collision Warning System for Small Maritime Autonomous Surface Ships", in *Journal of Marine Science and Technology*: Vol. 28: Iss. 6, Article 16. , 2020.
- [2] Lisowski, J. "Game control of moving objects." *IFAC Proc.* 35 (1), 373–378. , 2002.
- [3] F. Goerlandt, J. Montewka, V. Kuzmin and P. Kujala, "A risk-informed ship collision alert system", *Safety Science*, Volume 77, Pages 182-204, August 2015.
- [4] Jean-Francois Balmat, Frederic Lafont, Robert Maifret, Nathalie Pessel, "MARitime RiSk Assessment (MARISA), a fuzzy approach to define an individual ship risk factor" in *Ocean Engineering*, pp. 1278-1286, 2009.
- [5] P. Sotiralis, N.P. Ventikos, R. Hamann, P. Golyshev, A.P. Teixeira, "Incorporation of human factors into ship collision risk models focusing on human centred design aspects", *Reliability Engineering & System Safety* Volume 156, Pages 210-227, December 2016.
- [6] Tor Arne Johansen, Tristand Perez, and Andrea Cristofaro, "Ship Collision Avoidance and COLREGS Compliance Using Simulation-Based Control Behavior Selection With Predictive Hazard Assessment", in *IEEE Transactions on Intelligent Transportation Systems*, 2016.
- [7] C. Lee, D. Chung, J. Kim and J. Kim, "Nonlinear Model Predictive Control with Obstacle Avoidance Constraints for Autonomous Navigation in a Canal Environment", *IEEE/ASME Transactions on Mechatronics*, PP(99):1-12, January 2023.
- [8] S. Lefevre, D. Vasquez, C. Laugier, "A survey on motion prediction and risk assessment for intelligent vehicles", *ROBOMECH Journal* 1, July 2014
- [9] T. I. Fossen, "Handbook of marine craft hydrodynamics and motion control." John Wiley & Sons, 2011.
- [10] M. Huang, and D. Abel, "A*-guided incremental sampling for trajectory planning of inland vessels in narrow ship canals" in *2022 IEEE Intelligent Vehicles Symposium (IV)*, 2022, pp. 658-663.
- [11] O. Shyshova, P. Gadhavi, M. Tenzer, F. Tanshi, D. Söffker, "Takeover time: Requirements for highly automated inland vessels: First experimental-based results" *IEEE Conference on Cognitive and Computational Aspectsof Situation Management (CogSIMA)*, Montreal, Canada, May 7-10, 2024, accepted.
- [12] S. Helling, C. Roduner and T. Meurer, "On the dual implementation of collision-avoidance constraints in path-following mpc for underactuated surface vessels", in *2021 American Control Conference (ACC) 2021*, pp. 3366-3371.
- [13] M. M. Moser, M. Huang, and D. Abel, "Model Predictive Control for Safe Path Following in Narrow Inland Waterways for Rudder Steered Inland Vessels" *European Control Conference (ECC)*, 2023.
- [14] A. Ricci, "A constructive geometry for computer graphics," *The Computer Journal*, vol. 16, no. 2, pp. 157–160, 01 1973.
- [15] J. A. E. Andersson, J. Gillis, G. Horn, J. B. Rawlings, and M. Diehl, "CasADI – A software framework for nonlinear optimization and optimal control", *Mathematical Programming Computation*, vol. 11, no. 1, pp. 1–36, 2019.
- [16] A. W. L. T. Biegler, "On the implementation of an interior-point filter line-search algorithm for large-scale nonlinear programming", *Mathematical Programming*, vol. 106, 2006.